P-26

NASA CASE NO. NPO-19039-1-CU

PRINT FIG. 3b

NOTICE

The invention disclosed in this document resulted from research in aeronautical and space activities performed under programs of the National Aeronautics and Space Administration. The invention is owned by NASA and is, therefore, available for licensing in accordance with the NASA Patent Licensing Regulation (14 Code of Federal Regulations 1245.2).

To encourage commercial utilization of NASA-Owned inventions, it is NASA policy to grant licenses to commercial concerns. Although NASA encourages nonexclusive licensing to promote competition and achieve the widest possible utilization, NASA will consider the granting of a limited exclusive license, pursuant to the NASA Patent Licensing Regulations, when such a license will provide the necessary incentive to the licensee to achieve early practical application of the invention.

Address inquiries and all applications for license for this invention to NASA Patent Counsel, NASA Management Office-JPL, Mail Code 180-801, 4800 Oak Grove Drive, Pasadena, CA 91109-8099.

Approved NASA forms for application for nonexclusive or exclusive license are available from the above address.

Serial Number: 08/192,476

Filed Date: January 27, 1994

NMO-JPL

April 26, 1994

Serial No. 08/192,476
Filing Date January 27, 1994
Contract No. NAS7-1260
Contractor: Caltech/JPL
Pasadena, CA 91109-8099

RECONFIGURABLE OPTICAL INTERCONNECTIONS VIA DYNAMIC COMPUTER-GENERATED HOLOGRAMS

Inventors: Hua-Kuang Liu and
Shaomin Zhou

JPL Case No. 19039
Nasa Case No. NPO-19039-1-CU

Contractor: Jet Propulsion Laboratory

January 21, 1994

AWARDS ABSTRACT

The invention relates to improvements on a reconfigurable optical interconnection system of the type illustrated in **FIGs. 1** and **2** for parallel optical computing, neural networks, optical communications and similar applications where reconfigurable electrical interconnection patterns are employed.

FIG. 1(a) and **1(b)** illustrate the practical pixel spacing of a typical electrically-addressed spatial light modulator (ESLM) consisting of m=64 cells of width ***a*** and gaps of width ***b*** between adjacent cells. **FIG. 2(a)** illustrates conceptually the prior-art scheme for one-to-many regular reconfigurable optical interconnections, and **FIG. 2(b)** illustrates an optical implementation for that prior-art scheme where a single computer-generated hologram (CGH) stored in an ESLM is used to generate a regular array of interconnections using a single plane wave input beam.

An improved optical system illustrated conceptually in **FIG. 3(a)** for reconfigurable interconnections is achieved by providing dynamically programmable interconnections at an array of photodetectors placed at spatial points based on computer-generated holograms (CGHs) applied to an array of pixels of an electrically-addressed spatial light modulator (ESLM) using a plurality of light beams as illustrated in **FIG. 3(b)**. The criteria for computer-generation of the CGHs are array uniformity and diffraction efficiency, where uniformity is measured by a parameter which is defined as the root mean square of the intensities of the focal points in the array and diffraction efficiency is obtained by letting the sum of the powers in the signal spots of the array be divided by the total incident power. The optical system disclosed in **FIG. 3(b)** is for many spatial interconnections using an array of $K_1 \times K_1$ light beams where K_1 is an integer greater than one, preferably implemented by a single laser diode **10** and a multiple beam splitter (MBS) **14**, for illuminating through a Fourier transform lens **L** an array of $K_1 \times K_1$ areas of an ESLM, **13** each area being addressed by a sub-CGH from a computer **12'**. The combined output from $K_1 \times K_1$ sub-CGHs on the ESLM provides irregular interconnections at an array **11'** of light detectors positioned at N×N focal points on the output plane of the ESLM. By effectively placing a $K_1 \times K_1$ binary spatial filter **15** in the front of the ESLM, either as a discrete element or by incorporating it in the sub-CGHs, $2^{K1 \times K1}$ different irregular interconnection patterns may be provided. An optical system illustrated conceptually in **FIG. 4(a)** for many strength-adjustable interconnections comprises a plurality of laser sources **20**, 1xi(i=0,1...N-1), and a plurality of detectors **21**, 1xj(j=0,1...N-1), interconnected by an ESLM **23** with adjustable strength (weights) W_{ij} by

providing means for extending a linear array of N laser beams in one direction for illuminating each of N different columns of pixels in the ESLM, each of which is addressed by a sub-CGH to generate 1×j(j=0,1...N-1) beams that illuminate the N detectors positioned in a linear array optically orthogonal to the columns of pixels as shown in **FIG. 4(b)**. Optical means first Fourier transforms the 1×j(j=0,1...N-1) beams and then combines the N diffraction fields to form N individual beams for N interconnections. The strength of the interconnection sensed at each detector is given by

$$d_j = \sum_{i=0}^{N-1} W_{ji} S_i$$

where W_{ji} is the weight of the ji^{th} element in the interconnection weight matrix determined by the sub-CGHs which are readily adjustable in a computer used to generate the sub-CGHs.

FIG. 5 illustrates conceptually a cascaded three-stage crossover network (N=8) utilizing the many-to-many arrangement of **FIGs. 3(a)** and **3(b)** for each stage. **FIG. 6** is a graph of phase shift of a liquid crystal television (LCTV) ESLM versus applied voltage (from 0 to 0.35V) at two different wavelengths plotted by a dot for 632.8 nm and 514.5 nm. **FIGs. 7(a)** and **7(b)** illustrate computer simulation results for an example of one-to-two interconnection CGH using the 1st and 8th order outputs. **FIG. 7(a)** illustrates phase level distribution, and **FIG. 7(b)** illustrates diffraction field. The parameters are M=64, q=3:1, a=58 um, T_g=0.04, T_c=0.96, s=0.04, and ϕ_d=20°. **FIGs. 8(a)** and **8(b)** illustrate computer simulation results for an example of one-to-fourteen interconnection CGH using ±1, ±3, . . ., ±13 order outputs. **FIG. 8(a)** illustrates phase level distribution, and **FIG. 8(b)** illustrates diffraction field. The parameters are M=64, q=3:1, a=58 um, T_g=0.04, T_c=0.96, s=0.04, and ϕ_d=20°. **FIGs. 9(a)** and **9(b)** illustrate computer simulation results for an example of one-to-fifteen interconnection CGH using ±1, ±2, . . ., ±7 order outputs. **FIG. 9(a)** illustrates phase level distribution, and **FIG. 9(b)** illustrates diffraction field. The parameters are M=64, q=3:1, a=58 um, T_g=0.04, T_c=0.96, s=0.04, and ϕ_d=20°. **FIGs. 10(a)** and **10(b)** illustrate experimental results. **FIG. 10(a)** illustrates results for one-to-fourteen (±1, ±3, . . ., ±13 order outputs), and **FIG. 10(b)** illustrates results for one-to-fifteen (0, ±1, ±2, . . ., ±7 order outputs).

The novelty of the invention resides in the use of multiple beams for illuminating an ESLM that is comprised of a corresponding number of multiple ESLM areas addressed by a CGH or a number of sub-CGHs to produce reconfigurable patterns of interconnections at an array of detectors.

Serial No. 08/192,476
Filing Date January 27, 1994
Contract No. NAS7-1260
Contractor: Caltech/JPL
Pasadena, CA 91109-8099

JPL Case No. 19039
NASA Case No. NPO-19039-1-CU
F94125

PATENT APPLICATION

RECONFIGURABLE OPTICAL INTERCONNECTIONS VIA DYNAMIC COMPUTER-GENERATED HOLOGRAMS

ORIGIN OF INVENTION

The invention described herein was made in the performance of work under a NASA contract, and is subject to the provisions of Public Law 96-517 (35 USC 202) in which the contractor has elected not to retain title.

TECHNICAL FIELD

The invention relates to a reconfigurable optical interconnection system for parallel optical computing, neural networks, optical communications and similar applications where reconfigurable electrical interconnection patterns are employed.

BACKGROUND ART

Existing electronic interconnection techniques have several physical limitations, such as poor synchronization and low bandwidth, which cannot support the necessary interconnection density (for example, 10^{10} processing elements per integrated circuit chip, speed, for example, GaAs based processing elements operating at 100 MHz), and signal bandwidth requirements. To offer a possible solution to these problems, optical interconnection techniques have been suggested. [J.W. Goodman et al., Proc. IEEE, 72, 850 (1984) and A. Husain, SPIE **466**, 24, (1984)]

Noninterfering free-space optical interconnections possess the potential advantage of massive parallelism, high space bandwidth product (SBWP), high temporal bandwidth product (TBWP), low power consumption, low cross talk and low time skew as compared to electronic interconnections. Free-

space optical interconnection techniques have the further potential advantage that they can be used for both chip-to-chip and chip-to-module interconnections. Attention has been given to the use of various optical techniques, such as classical optics, diffraction optics, integrated optics, and holographic optics. For the purpose of implementing some important interconnection architectures, such as perfect shuffle [H.S. Stone, IEEE Trans. Comp., **C-20**, 153 (1971)], crossbar [M.A. Franklin, IEEE Trans. Comp., **C-30**, 283 (1981)], multistage interconnection networks (MINs), i.e., crossover networks [J. Jahns et al., Appl. Opt. **27**, 3155 (1988)], and Clos networks [C. Clos, Bell Syst. Tech. J., **32**, 406 (1953)], and other similar interconnection networks.

Recently, real-time reconfigurable optical interconnection techniques have been developed for parallel optical computing, neural networks, and optical communications using electrically-addressed spatial light modulators (ESLM) with computer-generated holograms (CGH). See, for example, A. Marrakchi et al., Opt. Lett. **16**, 931 (1991); E.C. Tam et al., Technical Digest of the OSA 1991 Annual Meeting, 146 (1991); J. Amako et al., Appl. Op. **30**, 4622, (1991); A. Varderlugt, SPIE **634**, 51 (1986). However, for this ESLM-CGH approach to become practical, higher throughput and more complicated interconnections will be required. For example, prior art shown implementations represented by U.S. patents 4,944,253; 5,115,497; 5,159,473 and 5,170,269 use a plane wave input beam and a single hologram. The latter patent relies on a deformable mirror device (DMD), which adds complexity to the otherwise reconfigurable interconnections but is otherwise also representative of the prior art that relies upon a single plane wave input beam and a single hologram to provide a reconfigurable pattern of interconnections. Such prior-art

approaches do not provide sufficient flexibility for a large enough interconnection network with high enough efficiency for large-scale practical use.

STATEMENT OF THE INVENTION

An optical system for providing dynamically programmable interconnections at an array at spatial points is based on computer-generated holograms (CGHs) applied to an array of pixels of an electrically-addressed spatial light modulator (ESLM).

The criteria for computer-generation of the CGHs are array uniformity and diffraction efficiency, where uniformity is measured by a parameter which is defined as the root mean square of the intensities of the focal points in the array and diffraction efficiency is obtained by letting the sum of the powers in the signal spots of the array be divided by the total incident power. An optical system for many spatial interconnections comprises an array of $K_1 \times K_1$ light beams where K_1 is an integer greater than one, preferably implemented by a single laser diode and a multiple beam-splitter (MBS), for illuminating through a Fourier transform lens L an array of $K_1 \times K_1$ areas of an ESLM, each area being addressed by a sub-CGH. The combined output from $K_1 \times K_1$ sub-CGHs on the ESLM provides irregular interconnection at an array of light detectors positioned at N×N focal points on the output plane of the ESLM. By effectively placing a $K_1 \times K_1$ binary spatial filter in the front of the ESLM, either as a discrete element or by incorporating it in the sub-CGHs, $2^{K1 \times K1}$ different irregular interconnection patterns may be provided.

An optical system for many strength-adjustable interconnections comprises a plurality of laser sources 1xi(i=0,1-...N-1) and a plurality of detectors 1xj(j=0,1...N-1)

interconnected by an ESLM with adjustable strength (weights) W_{ij} by providing means for extending a linear array of N laser beams in one direction for illuminating each of N different columns of pixels in the ESLM, each of which is addressed by a sub-CGH to generate 1×j(j=0,1...N-1) beams that illuminate the N detectors positioned in a linear array optically orthogonal to the columns of pixels. Optical means first Fourier transforms the 1×j(j=0,1...N-1) beams and then combines the N diffraction fields to form N individual beams for N interconnections. The strength of the interconnection sensed at each detector is given by

$$d_j = \sum_{i=0}^{N-1} W_{ji} S_i$$

where W_{ji} is the weight of the ji^{th} element in the interconnection weight matrix determined by the sub-CGHs which are readily adjustable in a computer used to generate the sub-CGHs.

BRIEF DESCRIPTION OF THE DRAWINGS

FIG. 1(a) and **1(b)** illustrate the practical pixel spacing of a typical electrically-addressed spatial light modulator (ESLM) consisting of m=64 cells of width ***a*** and gaps of width ***b*** between adjacent cells.

FIG. 2(a) illustrates conceptually the prior-art scheme for one-to-many regular reconfigurable optical interconnections, and **FIG. 2(b)** illustrates an optical implementation for that prior-art scheme where a single computer-generated hologram (CGH) stored in an ESLM is used to generate a regular array of interconnections using a single plane wave input beam.

FIG. 3(a) illustrates conceptually a one-to-many irregular reconfigurable interconnections to be achieved by the present invention for greater flexibility, and **FIG. 3(b)** illustrates an optical implementation of the irregular optical interconnections of **FIG. 3(a)**.

FIG. 4(a) illustrates conceptually a many-to-many (M×M) irregular reconfigurable optical interconnection network, and **FIG. 4(b)** illustrates an implementation of the M×M interconnection network of **FIG. 4(a)**.

FIG. 5 illustrates conceptually a three-stage crossover network (N=8) utilizing the many-to-many arrangement of **FIGs. 3(a)** and **3(b)** for each stage.

FIG. 6 is a graph of phase shift of a liquid crystal television (LCTV) ESLM versus applied voltage (from 0 to 0.35V) at two different wavelengths plotted by a dot for 632.8 nm and 514.5 nm.

FIGs. 7(a) and **7(b)** illustrate computer simulation results for an example of one-to-two interconnection CGH using the 1st and 8th order outputs. **FIG. 7(a)** illustrates phase level distribution, and **FIG. 7(b)** illustrates diffraction field. The parameters are M=64, q=3:1, a=58 μm, T_g=0.04, T_c=0.96, s=0.04, and ϕ_d=20°.

FIGs. 8(a) and **8(b)** illustrate computer simulation results for an example of one-to-fourteen interconnection CGH using ±1, ±3, . . ., ±13 order outputs. **FIG. 8(a)** illustrates phase level distribution, and **FIG. 8(b)** illustrates diffraction field. The parameters are M=64, q=3:1, a=58 μm, T_g=0.04, T_c=0.96, s=0.04, and ϕ_d=20°.

FIGs. 9(a) and **9(b)** illustrate computer simulation results for an example of one-to-fifteen interconnection CGH using ±1, ±2, . . ., ±7 order outputs. **FIG. 9(a)** illustrates phase level distribution, and **FIG. 9(b)** illustrates diffrac-

tion field. The parameters are M=64, q=3:1, a=58 μm, T_g=0.04, T_c=0.96, s=0.04, and ϕ_d=20°.

FIGs. 10(a) and **10(b)** illustrate experimental results. **FIG. 10(a)** illustrates results for one-to-fourteen (±1, ±3, . . ., ±13 order outputs), and **FIG. 10(b)** illustrates results for one-to-fifteen (0, ±1, ±2, . . ., ±7 order outputs).

DETAILED DESCRIPTION OF THE INVENTION

As shown in **FIGs. 1(a)** and **1(b)**, the practical pixel structure of a typical phase electrically-addressed spatial light modulator (ESLM) consists of cells of width *a* and gaps of width *b* between any two cells. There is also leakage in each cell. In the design of a computer-generated hologram (CGH) which is to be entered into an ESLM, the realistic pixel with leakage should be considered. If *m* pixels are selected as one period and *N* subpixels are taken within each pixel to calculate the Fourier spectrum of the profile, the complex amplitude transmittance in the case of one dimension may be expressed as

$$t_i = \begin{cases} T_g; & (m-1)N+\dfrac{a}{a+b}N+1 \le i < mN \\ T_c(1-s)e^{j(\varphi_d+\varphi_l)}+T_c s e^{j\varphi_d}; & (m-1)N \end{cases} \quad (1)$$

$$m=1,2,\ldots,M; i=1,2,\ldots,MN;$$

with

$$\varphi_l=\varphi_d+\frac{2\pi(l-1)}{L}; l=1,2,\ldots,L; \quad (2)$$

where s represents an assumed constant percentage of leakage, L is the phase level, T_c and T_g are the amplitude transmittances of the cell and gap, respectively, and φ_1 is the phase shift corresponding to L different phase levels. The phase shift of the gap and dark cell (l=1) are assumed to be zero and φ_d, respectively. In the implementation of the present invention, it is preferable to so prepare the CGHs that the transmittances of all cells are at the same T_c level, and only the phase shift is modulated.

The fast Fourier transform (FFT) algorithm is used to calculate the Fourier spectrum of Eq. (1), and annealing of the Fourier spectrum is achieved, such as by the simulated annealing iteration algorithm described by S. Kirkpatrick et al., Science, **220**, 671 (1983) incorporated herein by reference to obtain the desired diffraction patterns. There are two criteria for designing the CGH: (1) array uniformity and (2) diffraction efficiency [M.R. Feldman et al.,Opt. Lett., **14**, 479 (1989)]. The uniformity of the array is measured by a parameter which is defined as the root mean square error of the intensities of the focal points in the array. The diffraction efficiency is obtained by letting the sum of the powers in the signal spots of the array be divided by the total incident power.

An overall error mass function E is defined as follows:

$$E = E_1 + E_2 \qquad \textbf{(3a)}$$

$$E_1 = c_1\sqrt{\sum_{k=1}^{k}(I_k - I_0)^2} \tag{3b}$$

$$E_2 = c_2\left(\frac{n-1}{K}\right)^2 \tag{3c}$$

where I_k is the intensity of the kth diffraction order, I_0 is the mean value averaged over all the diffraction orders, K is the total number of the focal points in the array, and c_1 and c_2 are the optimization coefficients between zero and one. The desired array of spots may be designed based on an error tolerance (or a minimum tolerable error mass function) given *a priori*.

A two-dimensional CGH may be obtained by the superposition of two one-dimensional CGH structures. However, for increasing diffraction efficiency, a two-dimensional simulated annealing iteration algorithm may be used to search directly for an optimal two-dimensional CGH structure.

One-to-many regular interconnections

Reconfigurable one-to-many regular interconnections illustrated conceptually in prior-art **FIG. 2(a)** comprises a single laser light source **10** and an array (N×N, N=3) of detectors **11** that can be implemented directly by means of a single complex amplitude (or phase) computer-generated hologram (CGH) on an electrically-addressed spatial light modulator (ESLM) **13** which is illuminated by a laser light source **S**, e.g., a laser diode, through a Fourier transform lens **L**, as shown in **FIG. 2(b)**. N×N multiple focal points will be formed on detectors **11** positioned on the focal plane of the ESLM. The detectors illuminated by the light from the source transmitted through the ESLM under control of the CGH conduct

and thus provide interconnections between the two terminals of the detectors (photodiodes) at the spatial points of the array of detectors. The interval between two neighboring focal points can be controlled by changing the system parameters, such as object distance d_o, focal length of the lens, f, and the separation q between lens L and the ESLM.

One-to-many irregular interconnections

Reconfigurable one-to-many irregular interconnections, illustrated conceptually in **FIG. 3(a)** as again comprising a light source **10** and an array of detectors **11'**, may be implemented by providing a source of multiple beams, such as a fixed $K_1 \times K_1$ ($K_1=2$) multiple beam-splitter (MBS) **14** shown in **FIG. 3(b)**, to provide $K_1 \times K_1$ parallel channels that illuminate $K_1 \times K_1$ different **CGHs** from a digital computer **12'** on the spatial light modulator **13'**. Each channel provides a pattern of regular interconnections illustrated as being one pattern in each of four quadrants for the case of $K_1=2$, but the combination of these $K_1 \times K_1$ channels realize multiple irregular interconnections at an array of detectors **11'**. If a $K_1 \times K_1$ binary spatial filter array is placed in front or in back of the spatial light modulator **13'**, thereby producing a pattern of spots of no light onto the detectors from the spatial light modulator, whereby $2^{k1 \times k1}$ different irregular interconnection patterns (equal to 16 for the case of $K_1=2$) may be constructed by controlling the individual transmittance (opaque or transparent) in the filter array. The function of such a binary spatial filter **15** may be implemented in the digital computer by modifying the CGH generated according to the effect of the binary spatial filter superimposed on the CGH.

Strength-adjustable many-to-many interconnections

Strength-adjustable many-to-many interconnections, illustrated conceptually in **FIG. 4(a)** may be implemented as

shown in **FIG. 4(b)**. Referring first to **FIG. 4(a)**, a plurality of sources s_i (i=0,1,...N-1) and N detectors d_j (j=0,1,...N-1) interconnected with adjustable weights w_{ji}. Referring now to **FIG. 4(b)**, assume the same linear array arrangement of sources **20** and detectors **21**, but one oriented vertically and the other horizontally, although optical elements could be used to rotate the linear array of detectors 90° so they are oriented parallel to the linear array of the sources. The laser beams from the sources **20** are extended and collimated in the vertical direction by means of a spherical lens L_1 and a cylindrical lens CL_1 to illuminate **N** different columns of an electrically-addressed spatial light modulator (ESLM) **22**. Each column of the spatial light modulator is used to store a sub-CGH used to generate a 1xj (j=0,1,...N-1) beams. A set of spherical lens L_2 and cylindrical lens CL_2 is used to first Fourier transform the N sub-CGHs and then combine these N diffraction fields so that these N different sub-CGHs may form N individual beams for N interconnections. The power sensed at an output detector d_j may be written as

$$d_j = \sum_{i=0}^{N-1} w_{ji} s_i \qquad (4)$$

where w_{ji} is the ji^{th} element in the interconnection weight matrix (IWM) determined by the sub-CGHs which is, of course, adjustable in the computer **12** used to generate the sub-CGHs. In that manner, weighted interconnections between the two terminals of the detectors are provided at the spatial points where the detectors are positioned.

A variety of networks can be realized by the strength-adjustable many-to-many interconnection technique. Networks,

such as perfect shuffer and crossbar, may be implemented via a single layer strength-adjustable many-to-many interconnection. The multistage interconnection networks such as crossover [J. Jahns et al., Appl. Opt., 27, 3155 (1988), Clos [C. Clos, Bell Sys. Tech. J., 32, 406 (1953)], Benes [V. Benes, Bell Sys. Tech. J., 41, 1481 (1962)], Omega [D.H. Lawire, IEEE Trans. Comput., C-24, 1145 (1975)] and Baseline [C. Wu et al., IEEE Trans. Comput., C-29, 694 (1980)] may be implemented by cascading several strength-adjustable many-to-many interconnections. As an example, a three-stage crossover interconnection shown in FIG. 5 may be implemented as follows. The j^{th} output permutation of the power of the crossover may be represented as

$$d_j^{(1)} = s_j + s_{N-1-j} \tag{5a}$$

for the first stage where the stage number is denoted by the superscript in parenthesis "(1)", and N must be an integral power of two. The output of the first stage is used as input to the second stage. The permutation of the second stage output $d_j^{(2)}$ may be written as

$$d_j^{(2)} = \begin{cases} d_j^{(1)} + d_{N/2-j-1}^{(1)}; & 0 \le j \le N/2-1 \\ d_j^{(1)} + d_{3N/2-j-1}^{(1)}; & N/2 \le j \le N-1 \end{cases} \tag{5b}$$

For the third stage, the permutation of the output $d_j^{(3)}$ may be written as

$$d_j^{(3)} = \begin{cases} d_j^{(2)} + d_{N/4-j-1}^{(2)}; & 0 \le j \le N/4-1 \\ d_j^{(2)} + d_{3N/4-j-1}^{(2)}; & N/4 \le j \le N/2-1 \\ d_j^{(2)} + d_{5N/4-j-1}^{(2)}; & N/2 \le j \le 3N/4-1 \\ d_j^{(2)} + d_{7N/4-j-1}^{(2)}; & 3N/4 \le j \le N-1 \end{cases} \quad \textbf{(5c)}$$

For N=8, the first stage IWM may be written as

$$W^{(1)} = \begin{bmatrix} 1 & 0 & 0 & 0 & 0 & 0 & 0 & 1 \\ 0 & 1 & 0 & 0 & 0 & 0 & 1 & 0 \\ 0 & 0 & 1 & 0 & 0 & 1 & 0 & 0 \\ 0 & 0 & 0 & 1 & 1 & 0 & 0 & 0 \\ 0 & 0 & 0 & 1 & 1 & 0 & 0 & 0 \\ 0 & 0 & 1 & 0 & 0 & 1 & 0 & 0 \\ 0 & 1 & 0 & 0 & 0 & 0 & 1 & 0 \\ 1 & 0 & 0 & 0 & 0 & 0 & 0 & 1 \end{bmatrix} \quad \textbf{(6a)}$$

For the second stage,

$$W^{(2)} = \begin{bmatrix} 1 & 0 & 0 & 1 & 0 & 0 & 0 & 0 \\ 0 & 1 & 1 & 0 & 0 & 0 & 0 & 0 \\ 0 & 1 & 1 & 0 & 0 & 0 & 0 & 0 \\ 1 & 0 & 0 & 1 & 0 & 0 & 0 & 0 \\ 0 & 0 & 0 & 0 & 1 & 0 & 0 & 1 \\ 0 & 0 & 0 & 0 & 0 & 1 & 1 & 0 \\ 0 & 0 & 0 & 0 & 0 & 1 & 1 & 0 \\ 0 & 0 & 0 & 0 & 1 & 0 & 0 & 1 \end{bmatrix} \qquad \textbf{(6b)}$$

and for the third stage

$$W^{(3)} = \begin{bmatrix} 1 & 1 & 0 & 0 & 0 & 0 & 0 & 0 \\ 1 & 1 & 0 & 0 & 0 & 0 & 0 & 0 \\ 0 & 0 & 1 & 1 & 0 & 0 & 0 & 0 \\ 0 & 0 & 1 & 1 & 0 & 0 & 0 & 0 \\ 0 & 0 & 0 & 0 & 1 & 1 & 0 & 0 \\ 0 & 0 & 0 & 0 & 1 & 1 & 0 & 0 \\ 0 & 0 & 0 & 0 & 0 & 0 & 1 & 1 \\ 0 & 0 & 0 & 0 & 0 & 0 & 1 & 1 \end{bmatrix} \qquad \textbf{(6c)}$$

From these results, eight 1×2 strength-adjustable sub-CGHs of SBWP=8 are needed for each stage.

Computer simulations and experimental results

As noted with reference to **FIGs. 1(a),(b)** and **(c)** and **2(a),(b)**, the computer-generated holograms may be amplitude or phase, although amplitude CGHs are implied throughout. The following computer simulations and results were carried out with phase holograms for convenience in implementation of the computer program since they are equivalent and a Seiko-Epson liquid-crystal television (LCTV) ESLM operated in phase mode was available. First it was necessary to establish a look-up

table between the phase shift on the spatial light modulator ESLM and the applied voltage for phase control. **FIG. 6** gives the experimental result of the relationship between phase shift and applied voltage. The results of using a He-Ne laser and an Ar+ laser are shown. The dark phase φ_d was not considered in the figure. The phase shift is measured by means of a Mach-Zehnder interferometer. Other parameters of the LCTV are measured and the results are q=3:1, a=58μm, T_g=0.04 and s=4%. T_c is varied with an unexpected amplitude ±10% within the region from 0-3.5V because of the imperfect alignment of the liquid crystal molecules on the thin film transistor substrate [A. Marrakchi et al., (1991), *supra*]. An average value, T_c=0.96 is used in the computer simulations for simplifying the calculation process. The results of (a) pixel structures and (b) relative intensities for the computer simulation of several kinds of CGHs useful for making different interconnections are presented in **FIG. 7** through **FIG. 9**. **FIGs. 7(a)** and **7(b)** illustrate computer simulation results for an example of one-to-two interconnection CGH using the 1st and 8th order outputs. **FIG. 7(a)** illustrates phase level distribution, and **FIG. 7(b)** illustrates diffraction field. The parameters are M=64, q=3:1, a=58 μm, T_g=0.04, T_c=0.96, s=0.04, and ϕ_d=20°. **FIGs. 8(a)** and **8(b)** illustrate computer simulation results for an example of one-to-fourteen interconnection CGH using ±1, ±3, . . ., ±13 order outputs. **FIG. 8(a)** illustrates phase level distribution, and **FIG. 8(b)** illustrates diffraction field. The parameters are M=64, q=3:1, a=58 μm, T_g=0.04, T_c=0.96, s=0.04, and ϕ_d=20°. **FIGs. 9(a)** and **9(b)** illustrate computer simulation results for an example of one-to-fifteen interconnection CGH using ±1, ±2, . . ., ±7 order outputs. **FIG. 9(a)** illustrates phase level distribution, and **FIG. 9(b)** illustrates diffraction field.

The parameters are M=64, q=3:1, a=58 μm, T_g=0.04, T_c=0.96, s=0.04, and ϕ_d=20°. The experimental results demonstrating 1x14 and 1x15 interconnections are given in **FIG. 10(a)** and **10(b)**, which illustrate experimental results. **FIG. 10(a)** illustrates results for one-to-fourteen (±1, ±3, . . ., ±13 order outputs), and **FIG. 10(b)** illustrates results for one-to-fifteen (0, ±1, ±2, . . ., ±7 order outputs).

The consideration described above is based upon the assumption that **N** inputs are incoherent. However, if the input is a coherent source instead of the incoherent source array, constructive and destructive interference may affect the output. The power change caused by the interference on the vertical axis is not very significant if the ratio **R** between the horizontal dimension of the sub-**CGH** and the interval between the two nearest neighbor sub-**CGHs** is much less than one. For the same LCTV-ESLM, M=64, L=8, N=8, and R=0.1, computer simulation results show that the percentage decrease of the power is less than 5%.

RECONFIGURABLE OPTICAL INTERCONNECTIONS VIA DYNAMIC COMPUTER-GENERATED HOLOGRAMS

ABSTRACT OF THE DISCLOSURE

A system for optically providing one-to-many irregular interconnections, and strength-adjustable many-to-many irregular interconnections which may be provided with strengths (weights) w_{ij} using multiple laser beams which address multiple holograms and means for combining the beams modified by the holograms to form multiple interconnections, such as a cross-bar switching network. The optical means for interconnection is based on entering a series of complex computer-generated holograms on an electrically addressed spatial light modulator for real-time reconfigurations, thus providing flexibility for interconnection networks for large-scale practical use. By employing multiple sources and holograms, the number of interconnection patterns achieved is increased greatly.

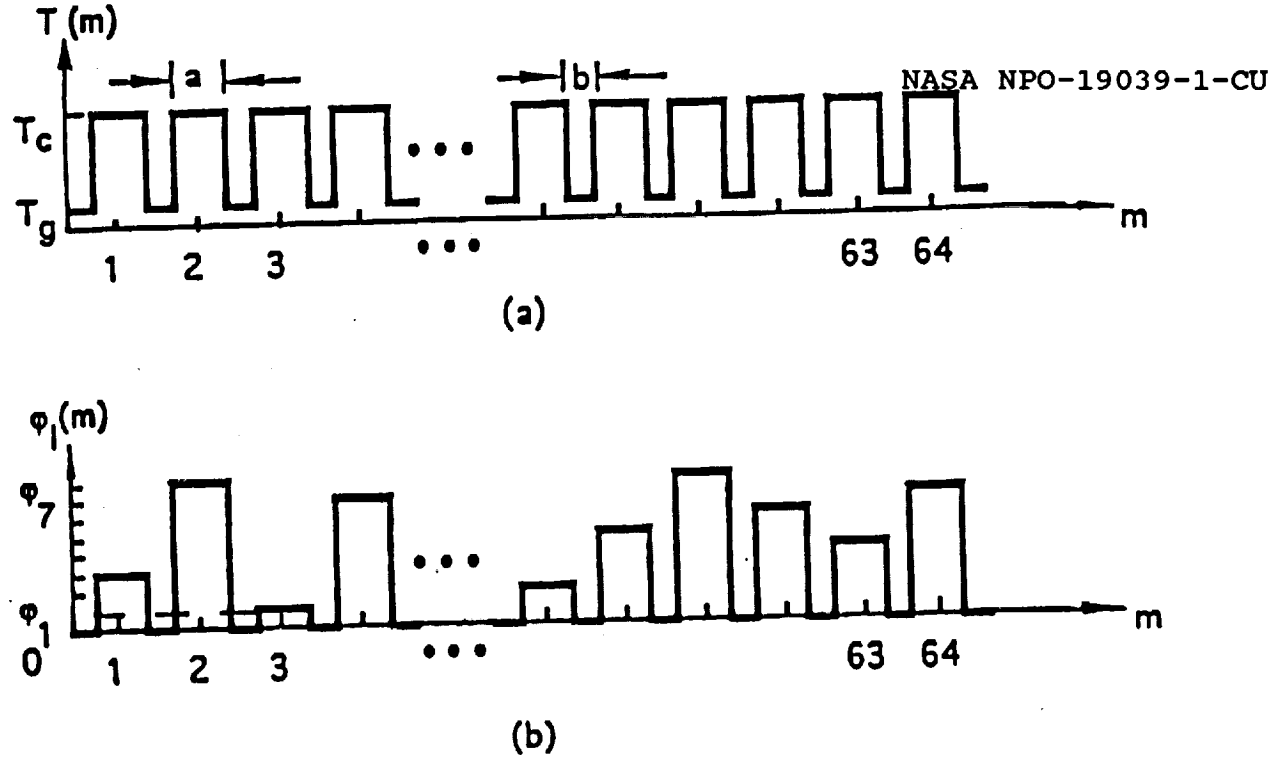

Fig.1

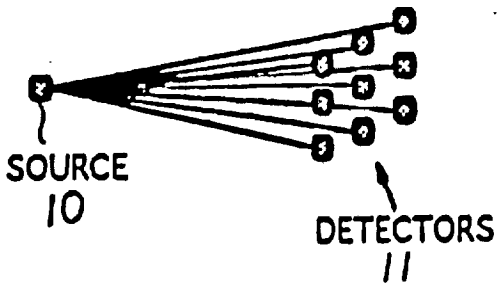

Fig.2 (a)

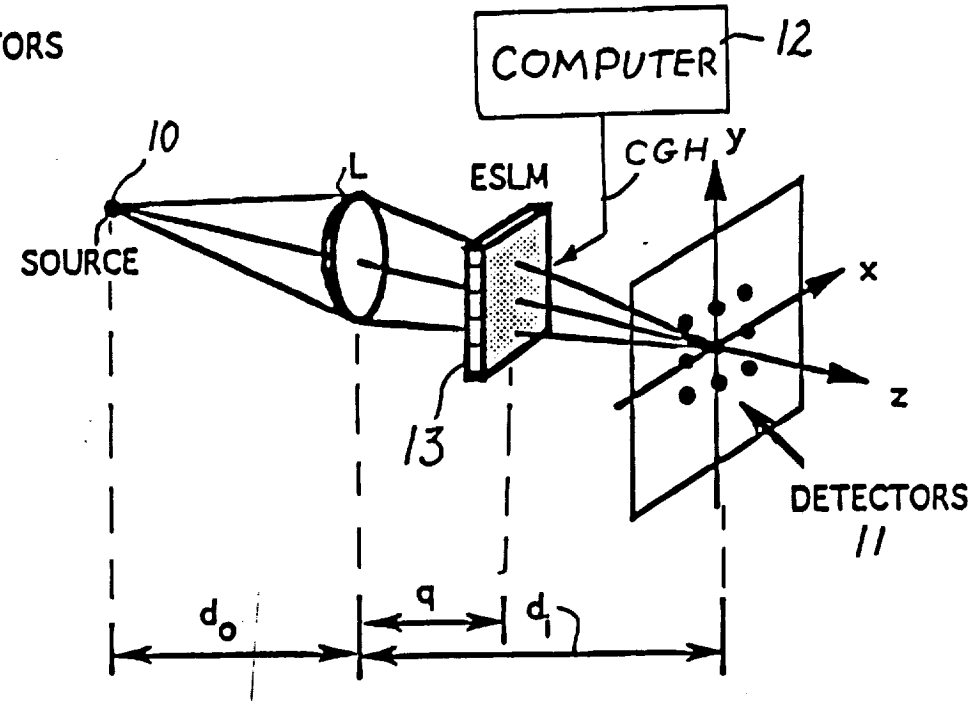

Fig.2 (b)

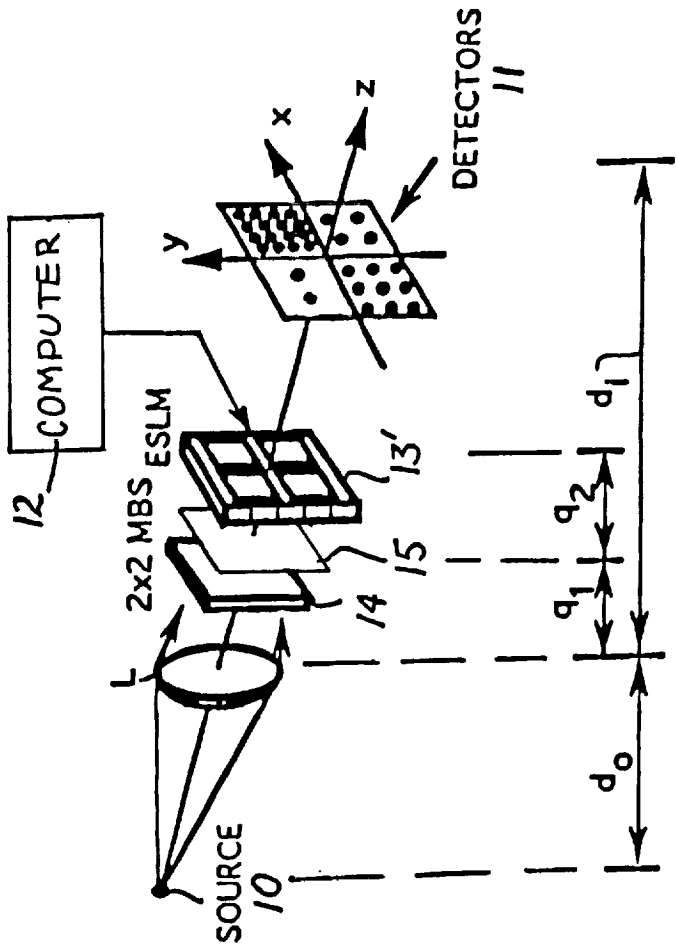
DETECTORS
11
x
z
y
COMPUTER
12
ESLM
13'
2x2 MBS
15
14
L
SOURCE
10
d_1
q_2
q_1
d_o

Fig.3 (b)

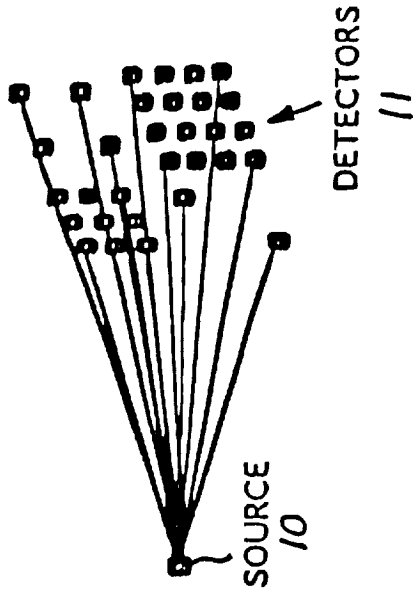
DETECTORS
11
SOURCE
10

Fig.3 (a)

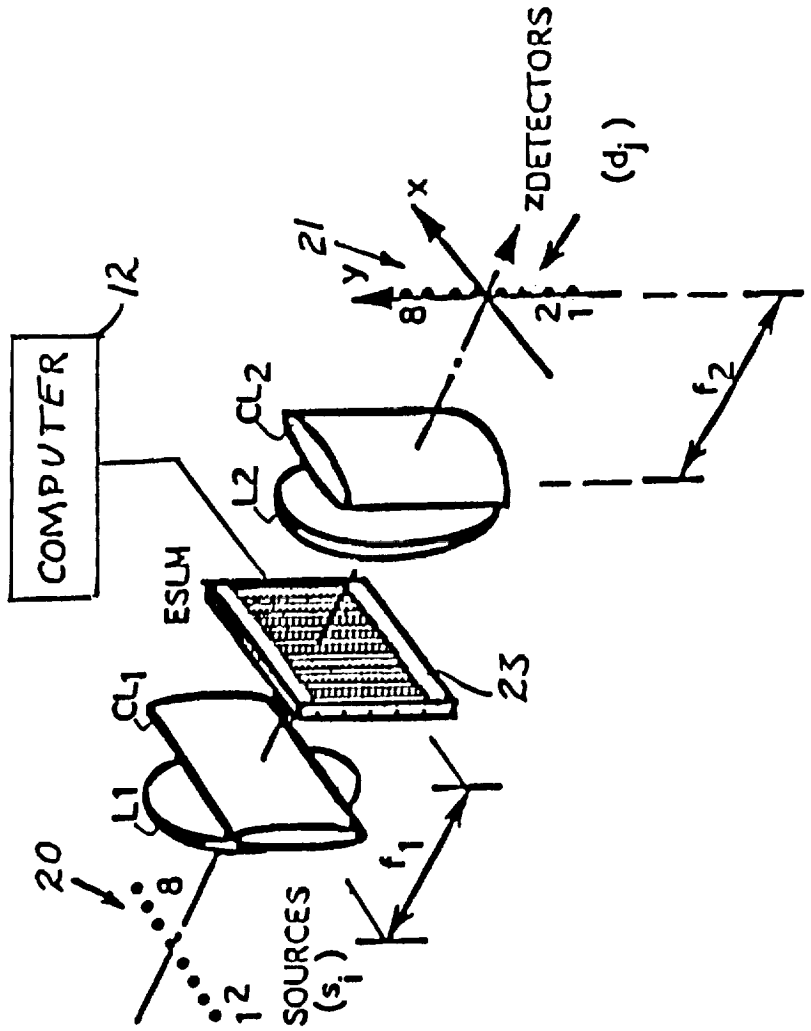
COMPUTER
12
ESLM
23
CL1
L1
CL2
L2
20
21
SOURCES
(s_i)
DETECTORS
(d_j)
f_1
f_2
x
y
z

Fig.4 (b)

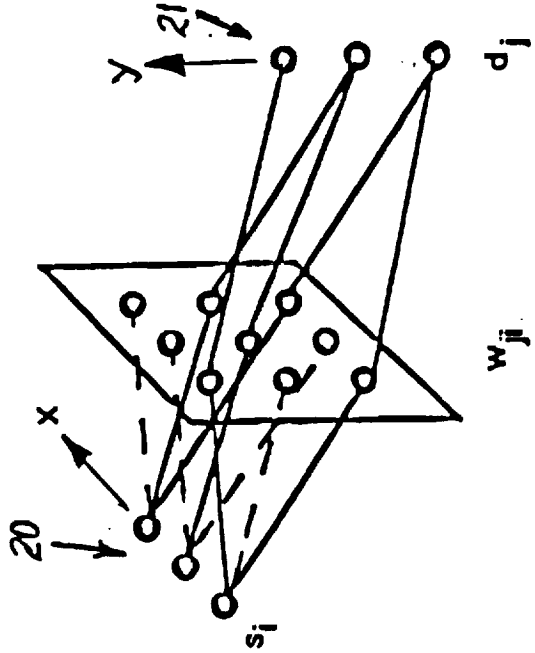
20
21
x
y
s_i
d_j
w_{ji}

Fig.4 (a)

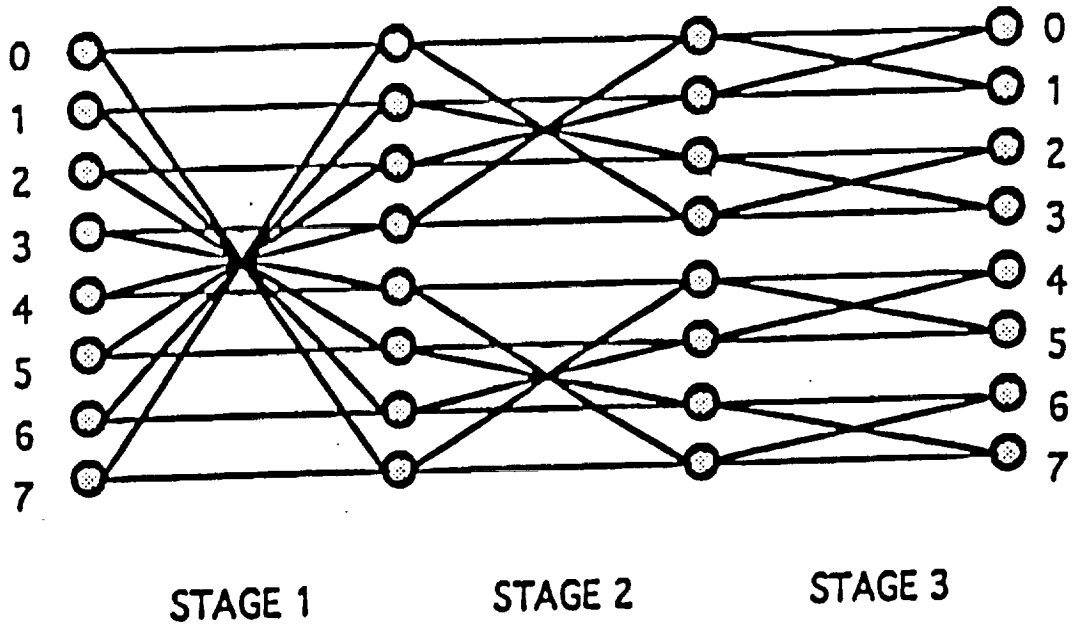
0
1
2
3
4
5
6
7
0
1
2
3
4
5
6
7
STAGE 1
STAGE 2
STAGE 3

Fig.5

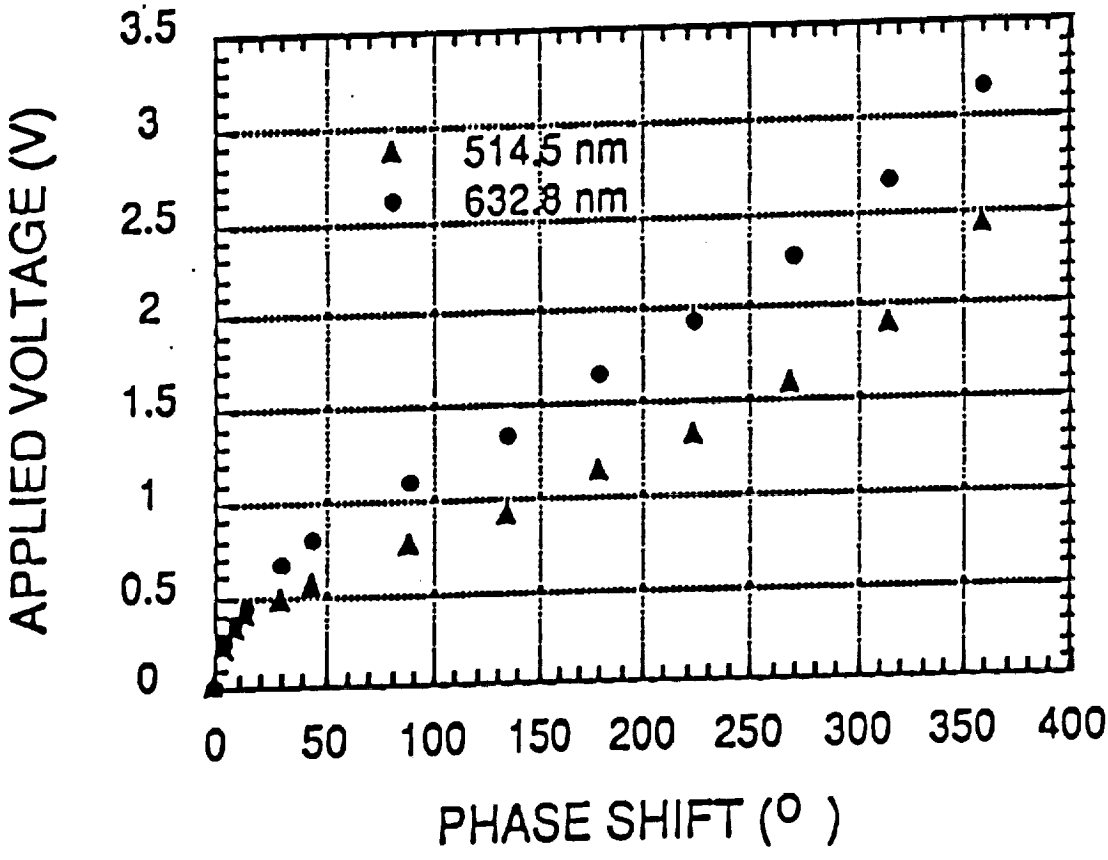
APPLIED VOLTAGE (V)
3.5
3
2.5
2
1.5
1
0.5
0
514.5 nm
632.8 nm
0
50
100
150
200
250
300
350
400
PHASE SHIFT (°)

Fig.6

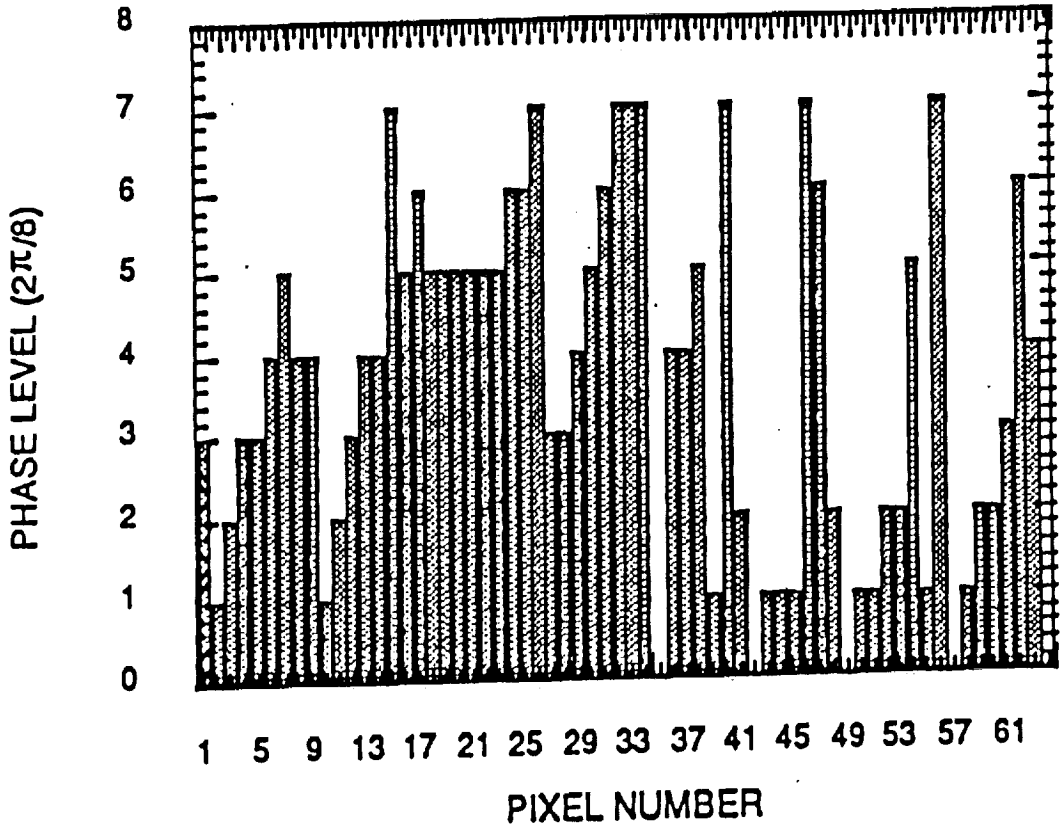
PHASE LEVEL (2π/8)
0
1
2
3
4
5
6
7
8
1 5 9 13 17 21 25 29 33 37 41 45 49 53 57 61
PIXEL NUMBER

Fig.7 (a)

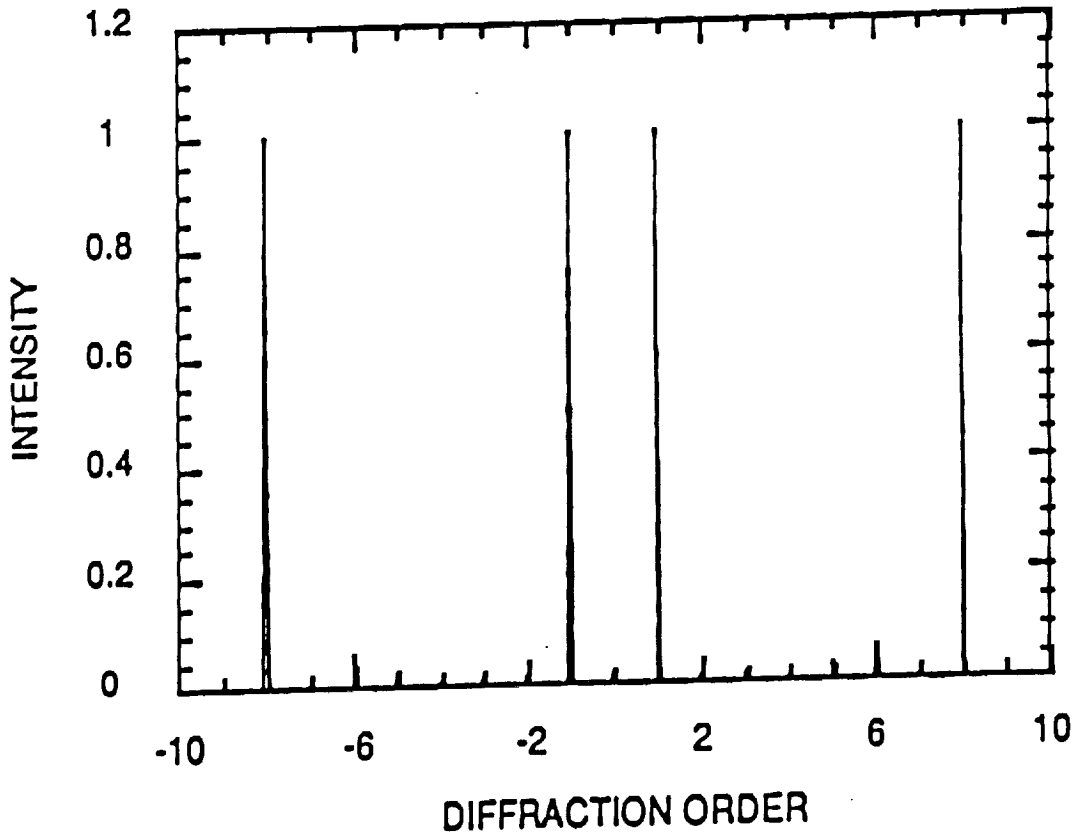
INTENSITY
0
0.2
0.4
0.6
0.8
1
1.2
-10 -6 -2 2 6 10
DIFFRACTION ORDER

Fig. 7 (b)

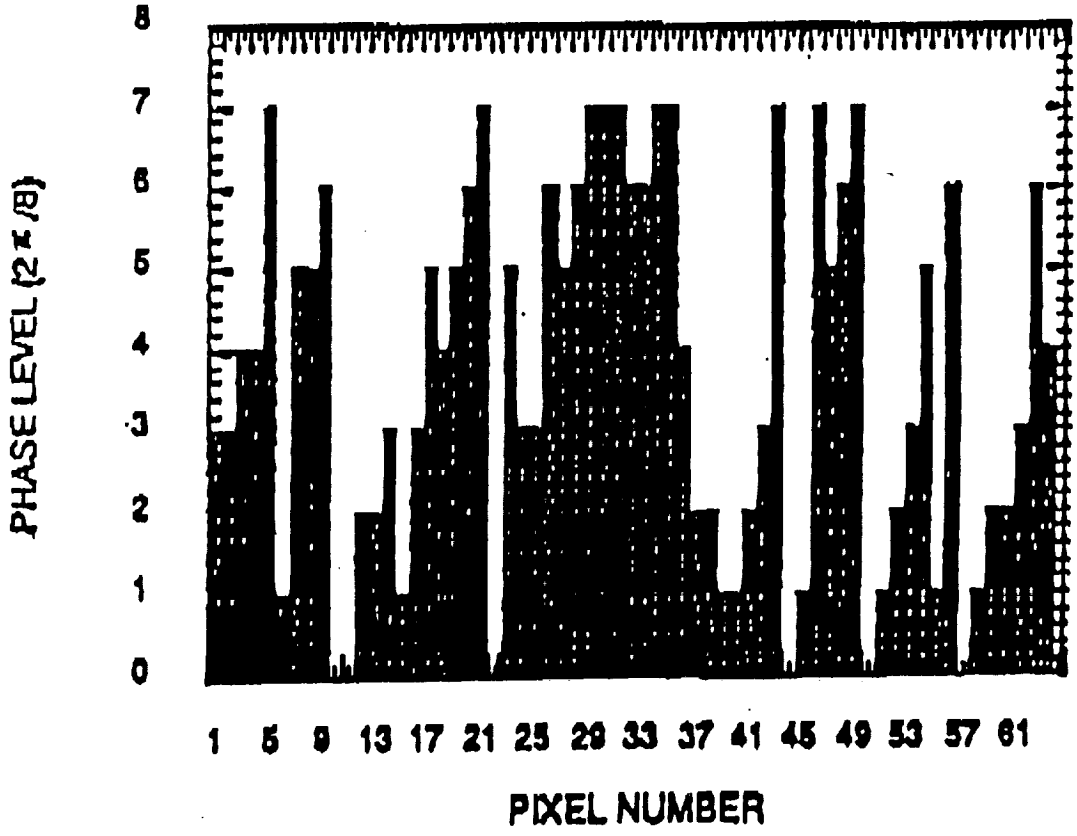
PHASE LEVEL (2π/8)
0
1
2
3
4
5
6
7
8
1 5 9 13 17 21 25 29 33 37 41 45 49 53 57 61
PIXEL NUMBER

Fig.8 (a)

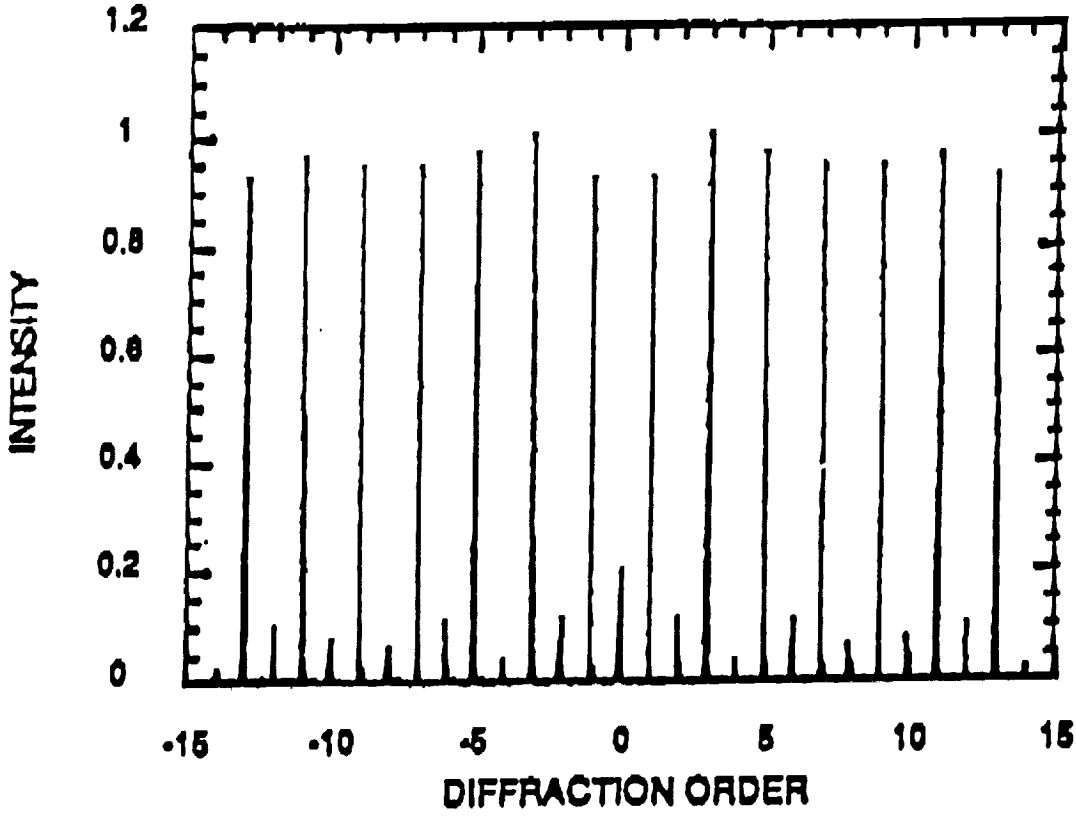
INTENSITY
0
0.2
0.4
0.6
0.8
1
1.2
-15 -10 -5 0 5 10 15
DIFFRACTION ORDER

Fig.8 (b)

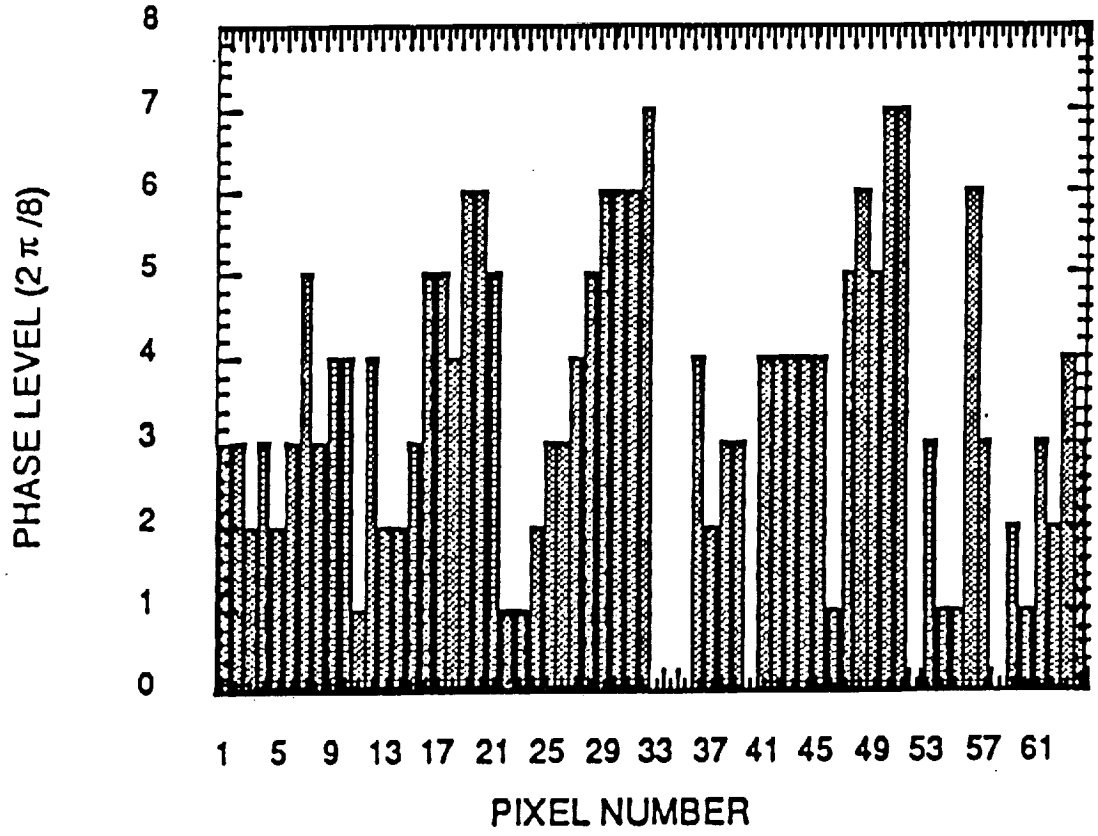
PHASE LEVEL (2π/8)
0
1
2
3
4
5
6
7
8
1 5 9 13 17 21 25 29 33 37 41 45 49 53 57 61
PIXEL NUMBER

Fig.9(a)

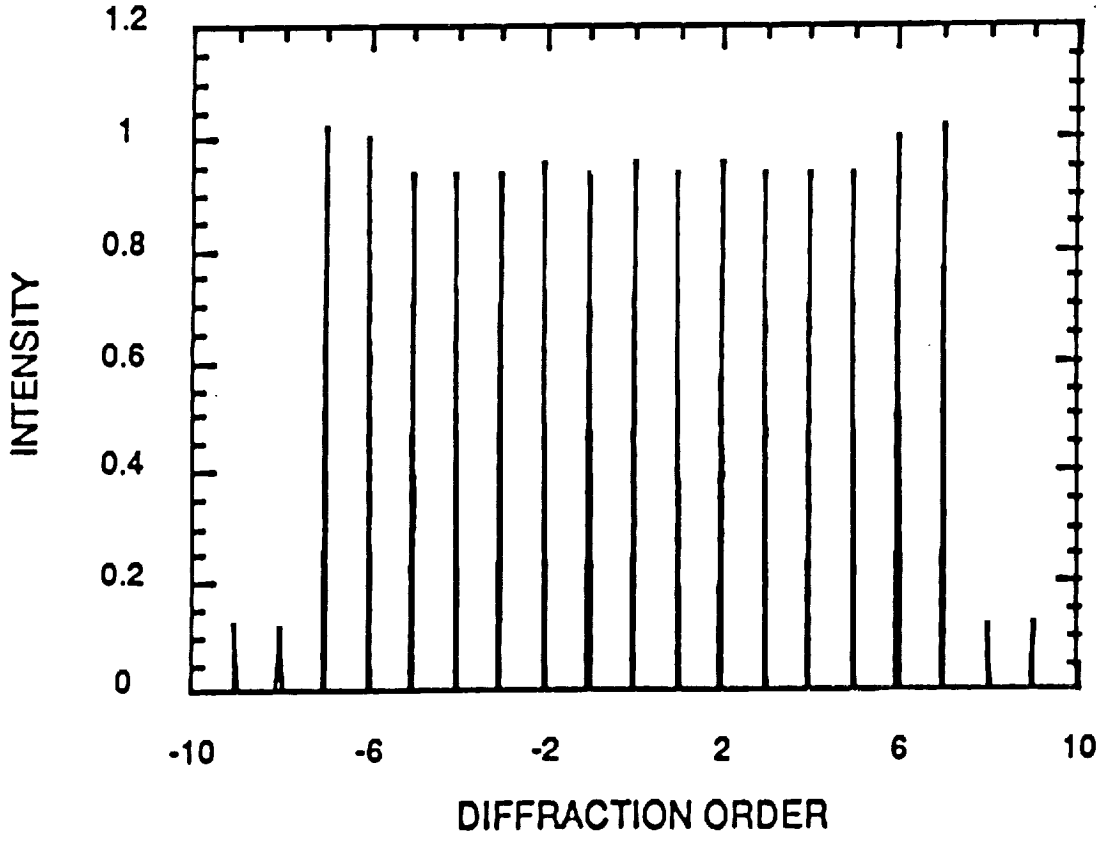
INTENSITY
0
0.2
0.4
0.6
0.8
1
1.2
-10 -6 -2 2 6 10
DIFFRACTION ORDER

Fig.9(b)

FIG. 10(b) 1X15

Fig.10(b) 1 x 15

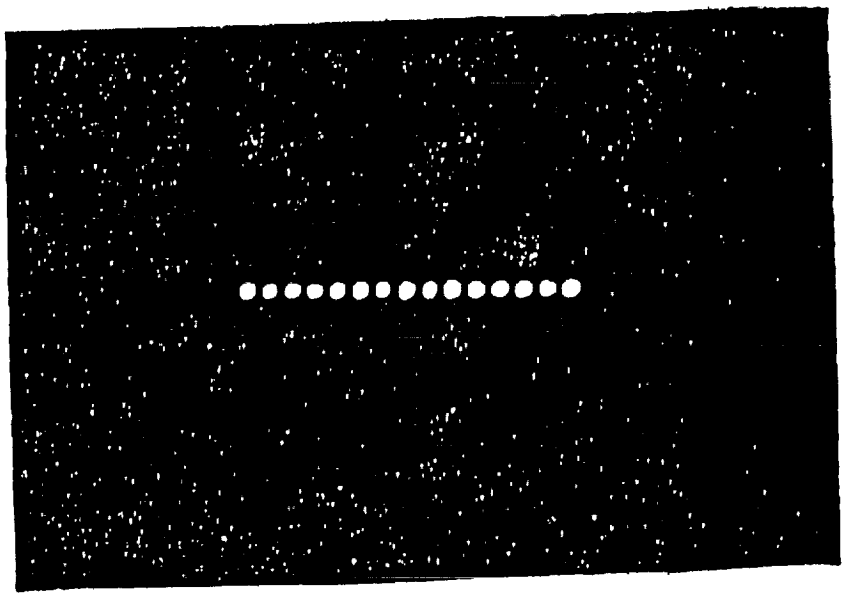

Fig.10 (a) 1 x 14

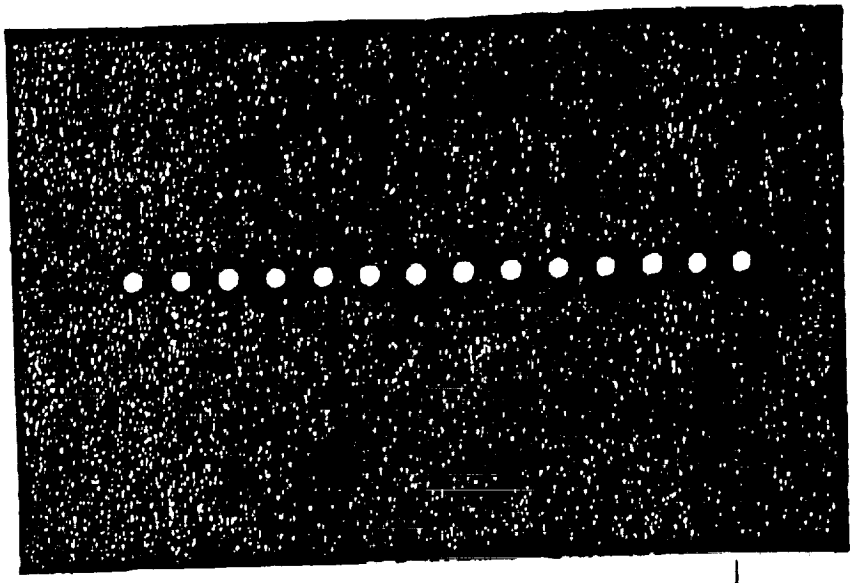

FIG. 10 (A) 1X14